Selection of Abnormal Trend in Nuclear β-decay Half-lives by Neural Network and Exploration of the Physical Mechanisms

Peng Li,[1,2] Zhong-Ming Niu,[3,*] and Yi-Fei Niu[1,2,†]

[1]*School of Nuclear Science and Technology, Lanzhou University,Lanzhou 730000, China*
[2]*Frontiers Science Center for Rare Isotopes, Lanzhou University, Lanzhou 730000, China*
[3]*School of Physics and Optoelectronic Engineering, Anhui University, Hefei 230601, China*

Nuclear β decay, as the typical decay process of unstable nuclei, is the key process for producing heavy elements in the universe. In this study, neural networks are employed to predict β-decay half-lives and for the first time to select the abnormal trend in nuclear β-decay half-lives based on deviations between experimental values and the predictions of neutral network. The nuclei with anomalous increases, abrupt peaks, sharp decreases, abnormal odd-even oscillations, and excessively large experimental errors in their β-decay half-lives, which deviate from systematic patterns, are identified through deviations. It is found that these anomalous phenomena might be associated with shell effects, shape coexistence, or discrepancies in experimental data. The discovery and analysis of these abnormal nuclei provide a valuable reference for further investigations with sophisticated microscopic theories, which may offer insights for uncovering new physics from the studies of nuclear β-decay half-lives.

Keywords: β-decay half-lives, Neural network, Abnormal nuclei

I. INTRODUCTION

"How were the elements from iron to uranium made?" This is a highly fascinating question and it has been listed in "Connecting Quarks with the Cosmos: Eleven Science Questions for the New Century" [1]. The rapid neutron capture processes (r-process) is responsible for producing roughly half of these heavy elements [2, 3], and it is the only mechanism for synthesizing elements heavier than bismuth [4]. One of the challenges in studying the r-process is obtaining precise nuclear physics inputs, such as nuclear mass, β-decay half-lives, neutron-capture cross sections and fission rate [5]. β decay, as the primary decay mode for most nuclei, plays a crucial role in determining the timescale of the r-process. It is predicted there are 9035 bound nuclides with proton numbers between 8 and 120 [6]. However, only about 3,000 nuclides have now been observed. [7]. Particularly for the nuclei far from the β-stability line, which are relevant to the r-process, current experimental data remain limited. Theoretical calculations not only guide experimental observations but also provide explanations for existing experiments, thereby advancing deeper understanding of the essence of matter and the laws of nature. Nevertheless, providing a precise description of the β-decay half-lives of nuclei is a great challenge because of the non-perturbative nature of nuclear forces and the complexity of quantum many-body problems.

Theoretical research on the β-decay half-lives can be broadly classified into empirical formula, gross theory and microscopic theory. Empirical formula is more appropriate for fitting experimental data and calculating various β-decay half-lives on a large scale [8, 9]. Compared to empirical formulas, gross theory can handle more complex situations and has a broader applicability [10–13]. Microscopic theory includes the shell model [14–18] and the quasiparticle random phase approximation (QRPA) model [19–29]. The shell model provides reliable predictions for β-decay half-lives, particularly for the nuclei in the light nuclear region and near magic numbers, but shell model calculations become increasingly challenging with the number of valence nucleons increasing. QRPA can calculate the β-decay properties of the vast majority of nuclei on the nuclear chart, except for a few light nuclei. Currently, when dealing with the nuclei lacking experimental data, researchers often employ the predictions of QRPA based on finite-range droplet model (FRDM+QRPA) [30–33] to provide inputs for r-process simulations.

In recent years, with the rapid progress of artificial intelligence, machine learning provides researchers with new approaches. Now the application of machine learning in the field of nuclear physics has become increasingly prominent [34], with applications in various areas, including making nuclear mass predictions [35–41], investigating charge radii [42–47], predicting the distribution of fission fragment yields in nuclei [48, 49], studying giant dipole resonances [50, 51], exploring excited states [52, 53] and other relevant topics [54–63].

The use of machine learning to study β-decay half-lives has also attracted widespread attention in recent years, and the predictive accuracy for β-decay half-lives has been continually improving [64–68]. Recently the machine learning predictions for the β-decay half-lives deviate from experimental values by only 2.24 times for nuclei with half-lives shorter than 10^6 seconds [67]. In this work, we propose a new application of neural network, with which the nuclei with deviations from

* Corresponding author, zmniu@ahu.edu.cn
† Corresponding author, niuyf@lzu.edu.cn

the systematic behavior in β-decay half-lives are identified. For those nuclei, machine learning cannot accurately describe the β-decay half-lives. Furthermore, theoretical models such as FRDM+QRPA [32, 33], relativistic Hartree-Bogoliubov + quasi-particle random phase approximation (RHB+QRPA) [26], gross theory based on WS4 mass model (WS4+GT) [13] predictions, and Skyrme-Hartree-Fock-Bogoliubov with the finite amplitude method (SHFB+FAM) [69] also encountered difficulties when attempting to describe these specific nuclei. After predicting β-decay half-lives and selecting these specific nuclei based on the deviations between experimental values and the predictions of neutral network, we analyzed the reasons for the challenges of neural network in describing the abnormal nuclei and explored the potential underlying physics.

II. NEURAL NETWORK MODEL

In this study, the neural network employed (Z, N, Q_β) as the inputs to predict β-decay half-lives and select the abnormal nuclei through deviations between experimental values and the predictions of neutral network, where Z, N, Q_β represent the proton number, the neutron number, and the β-decay energy, respectively. Q_β can be calculated from nuclear masses, which are taken from Bayesian Machine Learning (BML) model [37], since the root mean square error (RMSE) of the BML mass and the experimental values is only 84 keV. The output of neural network represents the logarithm of the β-decay half-life ($\log_{10} T_{1/2}$).

A total of 1072 nuclei from NUBASE2020 [7] were selected with $Z \geq 8$ and $N \geq 8$, β-decay half-lives less than 10^6 seconds and β-decay branching ratios greater than 10%. Therefore, the β-decay half-lives predicted by the neural network are less than 10^6 seconds. The experimental values for the majority of these 1072 nuclei are sufficiently precise. For example, the RMSE between the upper limits of the experimental values and their means was calculated to be only 0.056 orders of magnitude, which is significantly lower than the deviations in neural network and theoretical models. Therefore, it is observed that the larger deviations are isolated instances in a few specific nuclei, which require more precise measurements in future experiments. Similar to five-fold cross validation, the acquired data were randomly shuffled and divided into 5 parts, each containing 214, 214, 214, 214, and 216 nuclei, respectively. The first part of the data was used as the validation set, while the remaining parts served as the training set. Subsequently, the second part was employed as the validation set, and this process was iteratively repeated for the subsequent parts. This iterative process ensured that each nucleus was equally represented in both the training and validation sets, which differs from the neural networks employed in [67]. In this way, five sets of data were generated. Each of the five datasets was trained for 20,000 iterations, selecting the best 20 models per dataset, resulting in a total of 100 models. In the 20000 training iterations, different weight matrices were selected from a truncated normal distribution $\mathcal{N}(0, \sqrt{2/(h_{in}+h_{out})})$, where h_{in} and h_{out} represent the number of neurons on either end of the weight matrix [70]. Each training session used a different initial weight matrix and was iterated 50,000 times. The uncertainties of the neural network predictions were attributed to variations in the initial weight matrices. Subsequently, the mean of these 100 sets of predictions is denoted as the result of ANN1, with the standard deviation representing the uncertainties of the neural network predictions. Furthermore, guiding by the Bayesian neural network (BNN) approach, unequally weighted uncertainties of the predictions also can be supplied, with only slight differences from the uncertainties discussed in this study. And this small modification in uncertainties cannot affect our main conclusions. The $\sigma_{\rm rms}(\log_{10} T_{1/2})$] for ANN1 was calculated across various half-life intervals,

$$\sigma_{\rm rms}(\log_{10} T_{1/2}) = \sqrt{\frac{\sum_{i=1}^{n}(\log_{10} T_{1/2}^{\rm Exp} - \log_{10} T_{1/2}^{\rm ANN1})^2}{n}}. \tag{1}$$

To select the abnormal nuclei in the neural network, the nuclei across different magnitude levels of half-lives were selected where the neural network predictions deviate from experimental values by more than 1.96 times (95% confidence interval) the $\sigma_{\rm rms}(\log_{10} T_{1/2})$. Through this approach, 70 abnormal nuclei were selected. These abnormal nuclei were then excluded, and the same procedure of five-fold cross validation as adopted for ANN1 was applied to the remaining 1002 nuclei to obtain the results for ANN2.

In this study, a double-hidden-layer neural network was employed, which can be described by the following formula.

$$h_j^{[1]} = \text{softsign}(\sum_{i=1}^{n} \omega_{ij}^{[1]} x_i + b_j^{[1]}), \tag{2}$$

$$h_k^{[2]} = \text{softsign}(\sum_{j=1}^{H_1} \omega_{jk}^{[2]} h_j^{[1]} + b_k^{[2]}), \tag{3}$$

$$y = 6 * \tanh(\sum_{k=1}^{H_2} \omega_k^{[3]} h_k^{[2]} + b^{[3]}). \tag{4}$$

Here, x represents the inputs; ω and b represent the weight matrix and bias term; h indicates the hidden layer matrix; $H_1 = 29$ and $H_2 = 2$ signify the number of neurons in the first and second hidden layers; y represents the outputs. Since the FRDM+QRPA, RHB+QRPA, SHFB+FAM, and WS4+GT models predict half-lives greater than 10^{-4} seconds for all nuclei, in order to broaden the predictive range of the neural network, the predictions of the β-decay half-lives are set to be greater than 10^{-6} seconds.

After obtaining each value of y, the loss function Loss can be calculated,

$$\mathrm{Loss} = \frac{\sum_{i=1}^{m}(y_{\mathrm{Exp}} - y_{\mathrm{Pre}})^2}{m} + \frac{\lambda}{2}\sum_{j}\theta_j^2, \tag{5}$$

where y_{Exp} represents the experimental value from NUBASE2020; y_{Pre} represents the predictions of the neural network; θ represents the parameters of the neural network, including ω and b; m represents the number of data points in the training set, and λ is the hyperparameter for L_2 regularization (Tikhonov regularization [71, 72]), which can prevent neural network from overfitting and this is also an improvement compared to [67].

III. RESULTS AND DISCUSSION

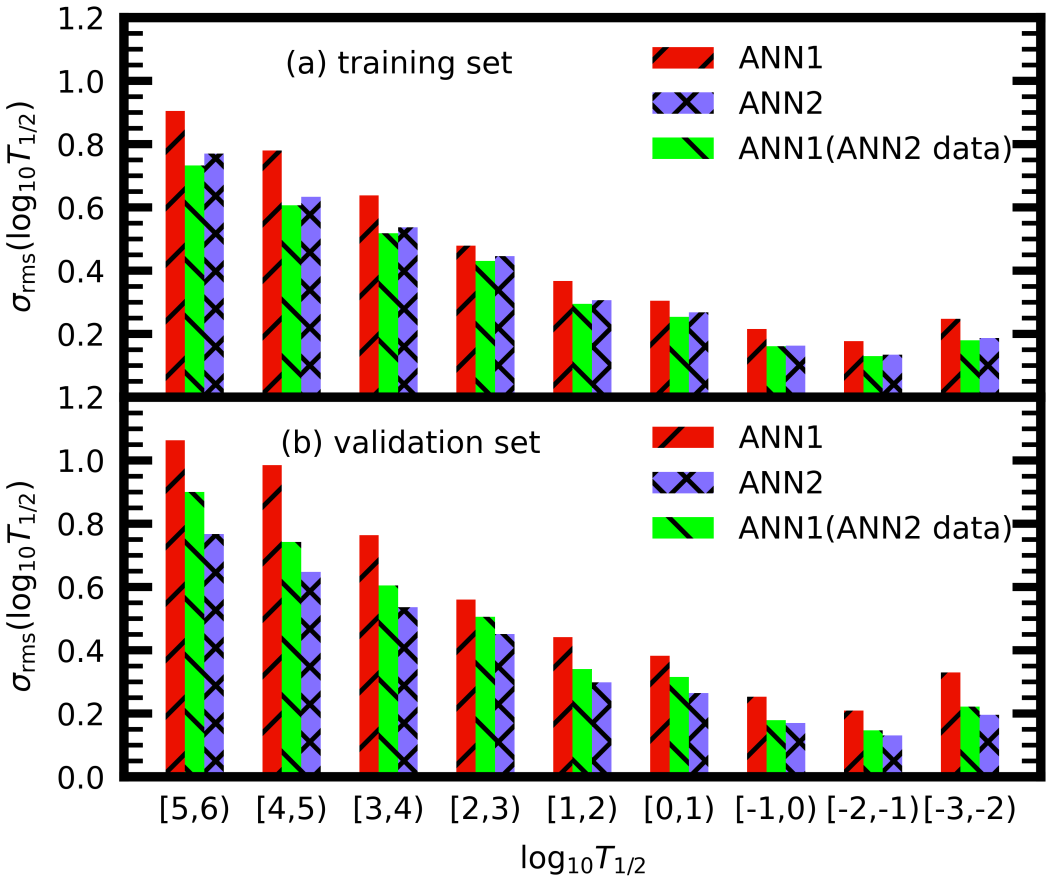

Fig. 1. The $\sigma_{\mathrm{rms}}(\log_{10}T_{1/2})$ across different half-life magnitudes between the predicted β-decay half-lives and experimental values for training set (a) and validation set (b), with each bar representing results for ANN1 on the entire dataset, ANN2 on the dataset excluding abnormal data, and ANN1 on the dataset excluding abnormal data.

Figure 1 shows the RMSE of predictions from both the ANN1 and ANN2 models across different half-life ranges. To allow for a clearer comparison of the predictions from ANN1 and ANN2, the RMSE values for ANN1, with abnormal nuclei excluded, are presented. It clearly shows that in most cases, the difference between the performances of both neural networks

on the training and validation sets is generally small, indicating that neither model exhibits overfitting. Additionally, figure 1 reveals that as nuclear half-lives decrease, the predictive accuracy of the neural network gradually improves, except for the nuclei with half-lives from the range of $10^{-2} \sim 10^{-1}$ seconds to $10^{-3} \sim 10^{-2}$ seconds. To allow for a clearer comparison of the predictions from ANN1 and ANN2, the RMSE values for ANN1, with abnormal nuclei excluded, are presented. ANN1, when excluding the selected 70 abnormal nuclei, exhibits prediction accuracy similar to ANN2, indicating that the selected nuclei behave differently from other nuclei.

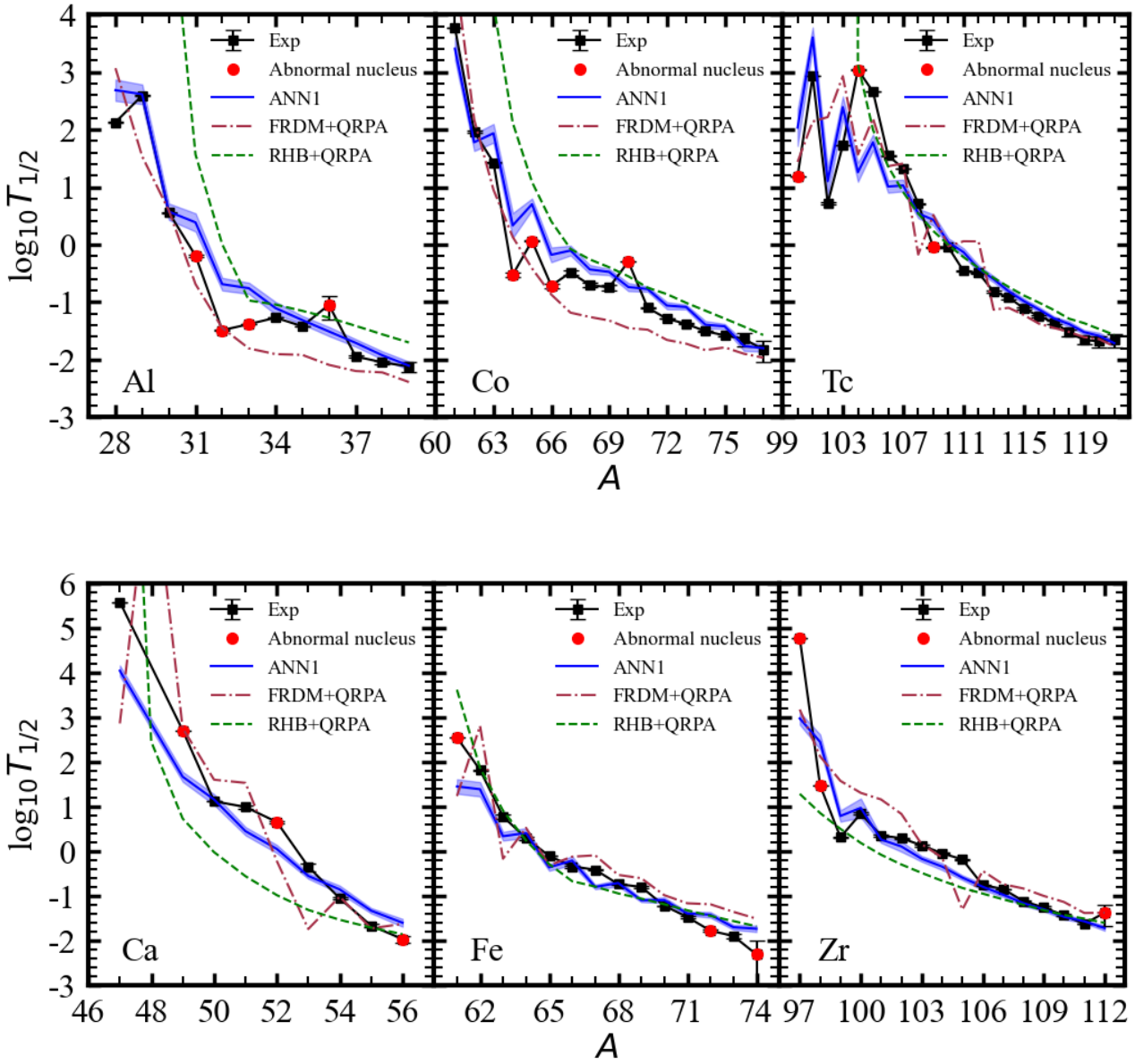

Fig. 2. Nuclear β-decay half-lives predicted by the neural network ANN1 for odd isotopes Al, Co, and Tc, as well as even isotopes Ca, Fe, and Zr along with corresponding 68% confidence interval error bars. The red points are the abnormal nuclei identified by ANN1. For comparison, theoretical results from the RHB + QRPA and FRDM + QRPA models are also presented.

Figure 2 shows typical abnormal nuclei picked up by the neural networks. The prediction of β-decay half-lives for nuclei in isotopic chains shows a smooth decrease as they move further from the β-stability line, which is consistent with experimental data. To better describe β-decay half-lives, in addition to the inputs (Z, N, Q_β), physical parameters such as the odd-even information δ ($\delta = (-1)^Z/2 + (-1)^N/2$), the deformation parameter β_2 and the variable related to the magic numbers P ($P = \nu_p\nu_n/(\nu_p + \nu_n)$ where ν_p and ν_n are the differences between Z, N and the nearest magic numbers) were introduced as inputs. However, incorporating these parameters did not significantly improve the predictions of the abnormal nuclei, and the extrapolations were worse than the presented results. From FIG. 2, it is evident that these nuclei display various anomalous

behaviors, such as: (1) Anomalous increases: with the neutron number increases, there is a notable increase in certain nuclear half-lives, particularly among nuclei ranging from ^{32}Al to ^{36}Al. (2) Sharp decreases: compared to surrounding nuclei, some nuclei display sharp decreases in their half-lives, such as ^{64}Co and ^{98}Zr. (3) Excessively large experimental errors: for some nuclei, experimental measurements of their half-lives come with relatively large errors, such as ^{36}Al and ^{74}Fe. (4) Abnormal odd-even oscillations: for specific nuclei, their β-decay half-lives exhibit odd-even oscillations distinct from typical patterns, such as ^{104}Tc. (5) Abrupt peaks: some nuclei display abrupt peaks in their behavior, setting them apart from the others, such as ^{70}Co and ^{36}Al. While the predictions of ANN1 for nuclei such as ^{28}Al, ^{106}Tc, and ^{47}Ca also exhibit significant deviations, this is due to the higher RMSE of ANN1 for nuclei with longer half-lives. However, the deviations between these predictions and the experimental values remain within 1.96 times RMSE for their intervals, and thus these nuclei were not classified as abnormal nuclei.

For these nuclei, the predictions of machine learning models show significant discrepancies compared to experimental data. However, accurately describing these isotopes remains quite challenging even when employing other theoretical models. For Al isotopes, FRDM+QRPA can accurately predict the β-decay half-lives of ^{31}Al and ^{32}Al, but it shows significant predictive deviation in the β-decay half-lives from ^{33}Al to ^{36}Al compared to experiment. Conversely, RHB+QRPA can provide more accurate predictions for the β-decay half-lives from ^{34}Al to ^{36}Al, but it shows notable disagreements in predicting the β-decay half-lives of other nuclei within the isotopes. Both models fail to reproduce the observed trend of anomalous increases in β-decay half-lives from ^{32}Al to ^{36}Al. For the Co isotopes, compared to neural networks, RHB+QRPA provides better β-decay half-lives predictions for ^{70}Co, however, for other nuclei within this isotopic chain, its predictive accuracy is not as well as that of neural networks. For FRDM+QRPA, it demonstrates better agreement with experiment for nuclei lighter than ^{66}Co compared to neural networks, but for nuclei heavier than ^{67}Co, its predictive accuracy is worse than that of neural networks. Moreover, predicting the β-decay half-life of ^{70}Co with FRDM+QRPA is particularly challenging. Both models also struggle to reliably predict all nuclei on the Co isotopes. For the other isotopes selected by FIG. 2, neither the FRDM+QRPA nor the RHB+QRPA models can accurately reproduce the beta-decay half-lives of the abnormal nuclei or their neighboring nuclei.

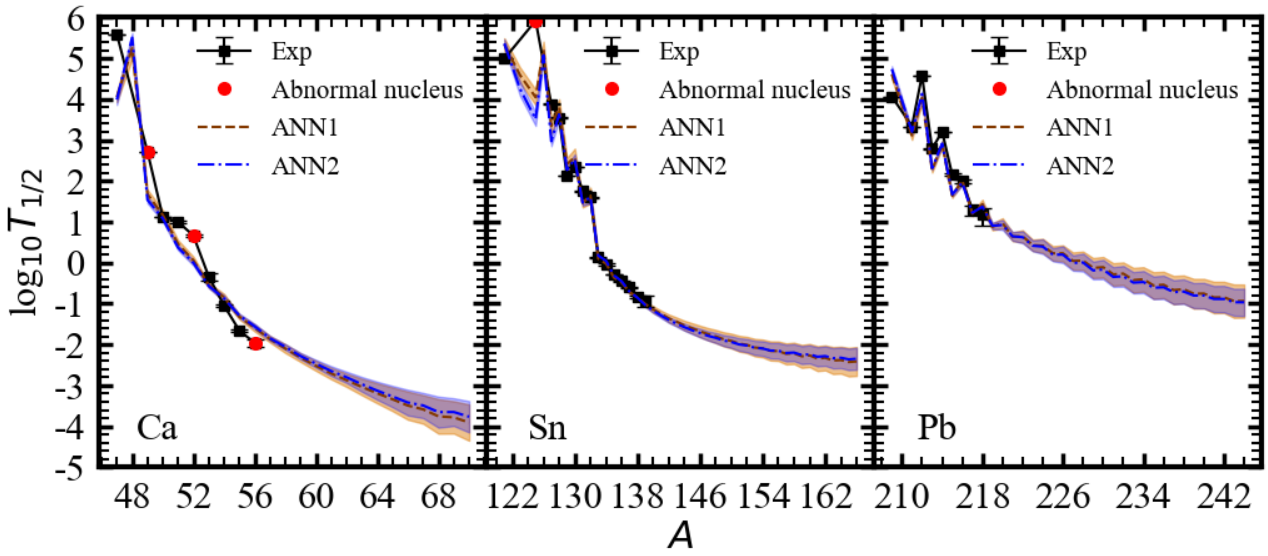

Fig. 3. Nuclear β-decay half-lives predicted by neural networks ANN1 and ANN2 for the Ca, Sn, and Pb isotopes along with corresponding 68% confidence interval error bars. The abnormal nuclei identified by the networks are indicated by red points. Experimental β-decay half-lives from NUBASE2020 are included for comparison.

In FIG. 3, the extrapolation results of two models are presented, accompanied by the 1σ (68% confidence interval) error bands. From FIG. 3, for nuclei with measured half-lives, it is found that the error bands of neural network are small, indicating a good agreement with the experimental data. For the nuclei selected by the neural network based on deviations between experimental values and the predictions of neutral network, both neural network models offer consistent results. Benefiting from training on the abnormal dataset, ANN1 achieves a slightly improved predictive performance. However, neither model is capable of providing precise descriptions of these abnormal nuclei. For nuclei without experimental values, ANN1 exhibits larger error bands. For all nuclei, it was found that the RMS between the means/upper bound/lower bound of ANN1 and ANN2 was 0.115/0.196/0.162 orders of magnitude, both models offer predictions that are very close, while the predictions of ANN1 are slightly shorter than the predictions of ANN2 for some cases.

Figure 4 provides a comparison between β-decay half-lives of isotones from ANN2 and other theoretical models. For nuclei

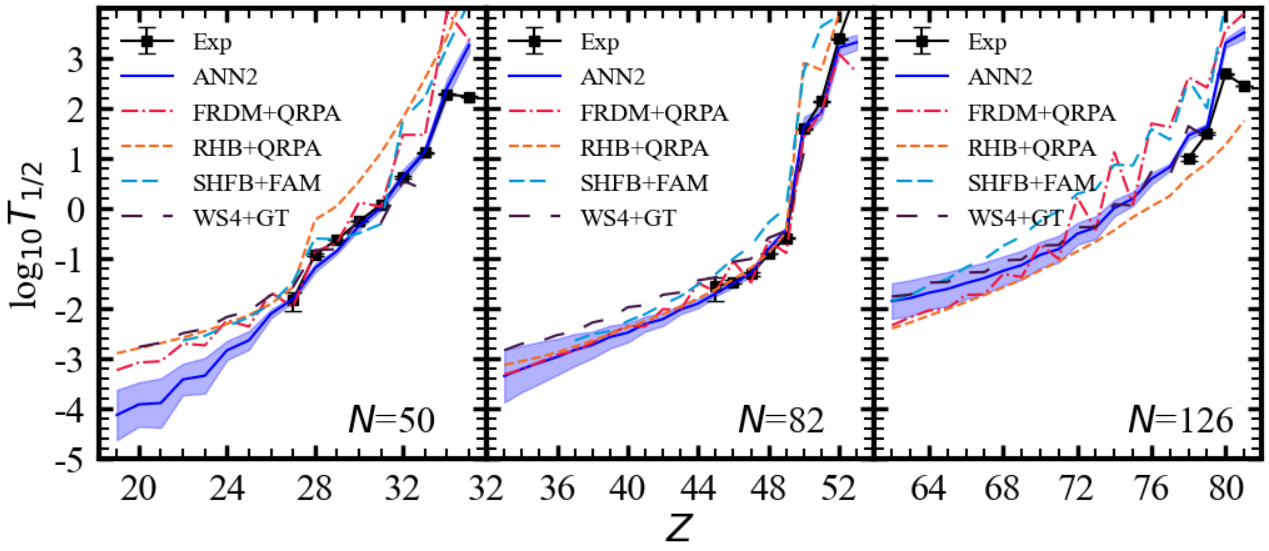

Fig. 4. β-decay half-lives of isotones predicted by ANN2 in comparison with the FRDM+QRPA, RHB+QRPA, SHFB+FAM, and WS4+GT results.

with experimental data, the predictions of neural network show better agreement with experimental results compared to those of other theoretical models. For the selected dataset of 1072 nuclei, the RMSE between the predictions of ANN1 and experimental values is 0.437, whereas the FRDM+QRPA shows an RMSE of 0.806 for these nuclei. Since the predictions of RHB+QRPA for some of the 1072 nuclei as stable, the predictions of RHB+QRPA for nuclei with half-lives shorter than 10^6s are compared, with an RMSE of 1.025 for 920 nuclei in this subset. Compared to those theoretical models, the neural network demonstrates higher predictive accuracy for β-decay half-lives. The neural network predicts shorter half-lives compared to other theoretical models in the neutron-rich region of $N = 50$ isotones. However, in the neutron-rich region of $N = 82$ and 126 isotones, the predictions from the neural network align more closely with those of other theoretical models, showing less disagreement.

Figure 5 shows the logarithmic differences between the β-decay half-lives predicted by ANN1 and the experimental values from NUBASE2020 for the 1072 nuclei selected in the dataset. The figure indicates that nuclei with significant deviations between the predictions of ANN1 and experimental values are concentrated near the β-stability line. For most nuclei (75.2%), the deviation between the predictions of ANN1 and experimental values is within 0.4 orders of magnitude. Among the 1072 nuclei β-decay half-lives, 548 (51.1%) were overestimated and 524 (48.9%) were underestimated by ANN1. ANN1 exhibited block alternations of overestimations and underestimations in predicting the β-decay half-lives of nuclei, accompanied by a certain degree of randomness. Neural networks tend to underestimate the β-decay half-lives of nuclei with magic numbers. For nuclei with magic numbers of protons or neutrons, 52 (58.4%) were underestimated and 37 (41.6%) were overestimated by ANN1. This suggests that the greater stability of magic nuclei presents additional challenges for neural networks in predicting their β-decay half-lives.

In FIG. 6, a concise analysis is provided to elucidate why the neural network encounters challenges in predicting certain nuclei. For ^{52}Ca, both the predictions of WS4 model and the values of experiment reveal a significant Δ_{2n} ($\Delta_{2n} = S_{2n}(Z,N) - S_{2n}(Z,N+2)$, where S_{2n} is the two-neutron separation energy) value for this nucleus, providing the evidence of shell effects. A recent article has also indicated that N=32 is a new magicity [74]. However, our neural network model does not incorporate this information, leading to reduced predictive accuracy for nuclei in this particular region. For ^{112}Zr, experimental measurements of its half-life come with relatively large uncertainties, which gives different results by treating the error bar differently. For example, NUBASE2020 reports a half-life of 43 ± 21 ms by taking a symmetric error bar. However, the original experimental measurement of the β-decay half-life for this nucleus is 30^{+20}_{-10} ms [75]. Future experimental measurements on the β-decay half-life of this nucleus with smaller error bars will help us understand this issue. For ^{97}Zr, ^{98}Zr, and ^{104}Tc, the β_2 data provided by the FRDM+QRPA and WS4 models [76] for nuclei in their vicinity show notable discrepancies. This divergence suggests the possible shape coexistence in these nuclei, which may contribute to explain the difficulties our neural network encounters when predicting nuclei in this particular region. The β-decay half-lives of these abnormal nuclei deviating from systematic patterns, may be better understood through in-depth investigations by more sophisticated models in the future. Such studies could contribute to uncovering new physics and thereby advancing our understanding of nuclear β decay.

The selected nuclei have been listed in the TABLE 1 along with their experimental half-lives and the predictions from ANN1 and ANN2. The abnormal nuclei includes 32 odd-odd nuclei, 26 odd-A nuclei, and only 12 even-even nuclei. Due to the presence of unpaired nucleons in odd nuclei, they exhibit more complex energy level structures, vibrational modes, and other

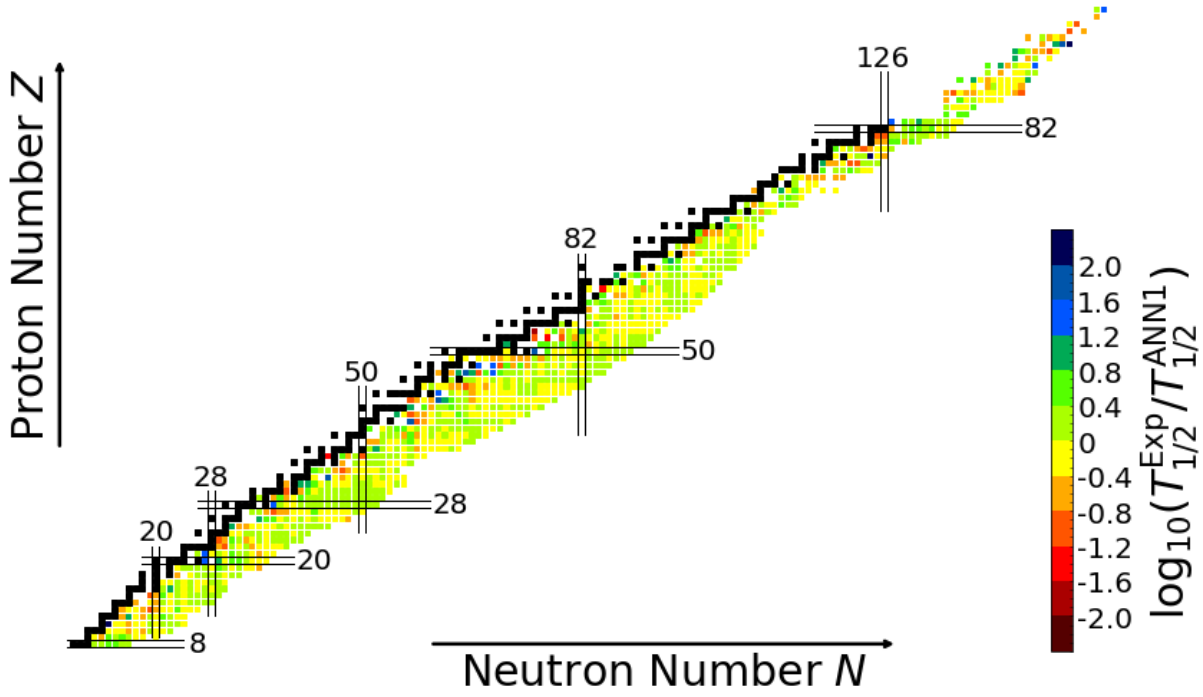

Fig. 5. The logarithmic difference distribution on nuclear chart between the predicted β-decay half-lives by ANN1 and experimental values, the black squares represent stable nuclei.

properties, making theoretical descriptions more challenging. For neural networks, although these methods are superior to traditional nuclear models in terms of representation capabilities, their performance is somewhat worse when dealing with odd nuclei compared to even ones. It also shows that the vital importance of physics in enhancing the performance of machine learning algorithms.

IV. SUMMARY AND OUTLOOK

In this work, a neural network was employed to predict β-decay half-lives and identify the nuclei whose β-decay half-lives deviate from systematic patterns based on deviations between experimental values and the predictions of neutral network. After excluding this subset of data, the models were retrained. Both neural network models exhibited similar $\sigma_{\rm rms}(\log_{10} T_{1/2})$, but the model trained on the original dataset displayed slightly larger error bands when extrapolating into the region of lighter nuclei. A brief analysis was also conducted to investigate the factors contributing to the challenges in predicting the half-lives of the selected nuclei. It appears that this challenge may be associated with the structural information of the nuclei that our neural network did not take into consideration. In the future, more sophisticated microscopic theoretical studies can help us comprehend the deeper physics within these abnormal nuclei, further advancing our understanding of β-decay. The neutral network integrating more suitable input parameters may enhance our capability to describe β-decay half-lives more effectively. It's also a good idea to sample the experimental values using the probability distribution function from the training data set. Although this method was not employed in this study due to the high precision of the experimental measurements of β-decay half-lives, we hope it will be employed in future nuclear physics research. Neural networks were employed to directly learn the experimental values of nuclear β-decay half-lives by taking the known variables related to β-decay half-lives (Z, N, Q_β) as inputs. High prediction accuracy for β-decay half-lives has been achieved by this approach without considering other theoretical factors. The β-decay half-life anomalies identified through the neural network method represent currently unexplained information about β-decay, which may offer insights for discovering new physics in the future. Machine learning methods such as Density-Based Spatial Clustering of Applications with Noise (DBSCAN), K-Nearest Neighbors (KNN), and other algorithms also can be employed to identify abnormal nuclei, potentially offering new insights into anomalous phenomena in nuclear β-decay half-lives. We hope that in the future, more suitable machine learning methods would be used to identify abnormal nuclei.

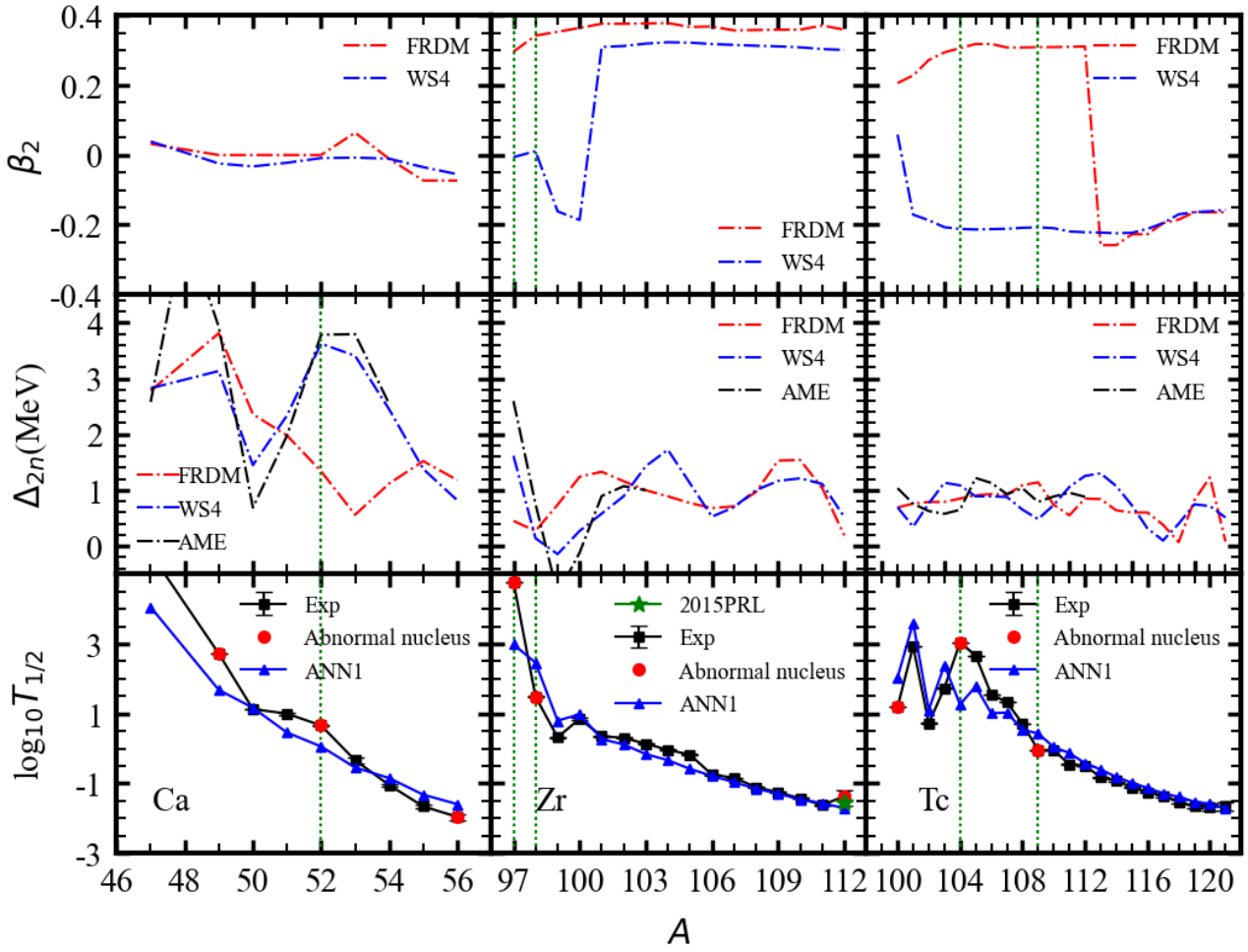

Fig. 6. The predictions of ANN1 and the value of experiment of $\log_{10} T_{1/2}$ for Ca, Zr, and Tc isotopes including abnormal nuclei are shown, along with quadrupole deformation β_2 from FRDM and WS4 models. Additionally, the two-neutron shell gap Δ_{2n} values from the FRDM and WS4 predictions, as well as from AME [73] experimental values, are provided.

V. ACKNOWLEDGMENTS

This work was partly supported by the 'Young Scientist Scheme' of the National Key R&D Program of China (Contract No. 2021YFA1601500), the National Natural Science Foundation of China under Grants No. 12075104, No. 12375109, No. 11875070, and No. 11935001, the Anhui project (Z010118169), and the Key Research Foundation of the Education Ministry of Anhui Province under Grant No. 2023AH050095.

[1] National Research Council, in Connecting quarks with the cosmos: eleven science questions for the new century (The National Academies Press, Washington, 2003)
[2] M. Sasano, G. Perdikakis, R. G. T. Zegers *et al.*, Gamow-Teller Transition Strengths from ^{56}Ni, Phys. Rev. Lett. **107**, 202501 (2011). doi: 10.1103/PhysRevLett.107.202501
[3] E. Margaret Burbidge, G. R. Burbidge, W. A. Fowler *et al.*, Synthesis of the Elements in Stars, Rev. Mod. Phys. **29**, 547 (1957). doi: 10.1103/RevModPhys.29.547
[4] F. Käppeler, R. Gallino, S. Bisterzo *et al.*, The s process: Nuclear physics, stellar models, and observations. Rev. Mod. Phys. **83**, 157 (2011). doi: 10.1103/RevModPhys.83.157
[5] M. Arnould, S. Goriely, and K. Takahashi, In-medium nuclear interactions of low-energy hadrons, Phys. Rep. **450**, 97 (2007). doi: 10.1016/j.physrep.2007.08.002

TABLE 1. The selected nuclei with abnormal trends in nuclear β-decay half-lives by neural network, along with their experimental β-decay half-lives and the predictions from ANN1 and ANN2.

Z	N	$\log_{10}(T_{1/2}^{\rm Exp})$	$\log_{10}(T_{1/2}^{\rm ANN1})$	$\log_{10}(T_{1/2}^{\rm ANN2})$	Z	N	$\log_{10}(T_{1/2}^{\rm Exp})$	$\log_{10}(T_{1/2}^{\rm ANN1})$	$\log_{10}(T_{1/2}^{\rm ANN2})$
9	13	0.626	-0.094	-0.467	33	48	1.522	2.272	2.384
9	15	-0.416	-1.200	-1.379	35	45	3.063	4.390	4.757
10	16	-0.706	-0.193	0.063	35	50	2.241	3.269	3.242
10	17	-1.510	-1.132	-1.105	40	57	4.780	2.983	2.936
10	18	-1.726	-1.198	-1.127	40	58	1.487	2.460	2.387
11	13	4.731	1.972	1.446	40	72	-1.367	-1.713	-1.687
11	16	-0.521	-0.042	0.040	41	57	0.456	1.456	1.699
11	17	-1.480	-1.121	-1.122	41	58	1.176	1.964	2.390
12	18	-0.499	0.051	0.445	42	63	1.560	0.820	0.752
12	20	-1.095	-0.743	-0.565	43	57	1.189	2.036	2.407
12	21	-1.036	-1.472	-1.338	43	61	3.041	1.261	0.922
13	18	-0.191	0.388	0.690	43	66	-0.043	0.432	0.388
13	19	-1.487	-0.686	-0.458	45	64	1.907	2.655	2.857
13	20	-1.382	-0.758	-0.517	45	65	0.525	1.411	1.153
13	23	-1.046	-1.509	-1.502	45	66	1.041	1.819	1.871
14	20	0.442	1.075	1.508	47	65	4.052	2.101	1.386
15	19	1.094	2.117	2.145	47	67	0.663	1.507	0.982
19	35	-2.000	-1.543	-1.508	47	69	2.361	1.090	0.861
20	29	2.719	1.678	1.537	50	75	5.920	4.046	3.512
20	32	0.663	0.060	0.000	51	83	-0.171	0.439	0.544
20	36	-1.959	-1.593	-1.555	52	77	3.621	5.005	5.330
21	35	-1.585	-1.101	-1.058	53	75	3.207	5.067	5.702
23	33	-0.666	-0.140	0.132	59	85	3.016	4.331	4.721
25	37	-1.036	-0.649	-0.473	75	119	0.699	1.315	1.420
26	35	2.555	1.461	1.399	77	119	1.716	2.451	2.769
26	46	-1.770	-1.414	-1.373	77	121	0.940	1.761	1.982
26	48	-2.301	-1.727	-1.671	77	122	0.845	1.742	1.914
27	37	-0.523	0.335	0.640	78	124	5.200	2.528	2.509
27	38	0.064	0.704	0.757	79	123	1.453	2.338	2.618
27	39	-0.712	-0.176	0.082	79	124	1.778	2.509	2.642
27	43	-0.294	-0.737	-0.658	81	125	2.402	3.485	3.697
28	37	3.957	2.658	2.211	81	126	2.457	3.525	3.648
29	39	1.490	2.287	2.436	87	146	-0.046	1.115	1.128
32	45	4.606	2.889	2.754	91	148	3.812	2.348	2.151
33	47	1.182	2.168	2.505	94	153	5.293	2.939	2.625

[6] X. W. Xia, Y. Lim, P. W. Zhao *et al.*, The limits of the nuclear landscape explored by the relativistic continuum Hartree–Bogoliubov theory, At. Data Nucl. Data Tables **121-122**, 1 (2018). doi: 10.1016/j.adt.2018.02.001

[7] F. G. Kondev, M. Wang, W. J. Huang *et al.*, The NUBASE2020 evaluation of nuclear physics properties, Chin. Phys. C **45**, 030001 (2021). doi: 10.1088/1674-1137/abddae

[8] Y. Zhou, Z. H. Li, Y. S. Chen *et al.*, Estimate of β^--decay Half-lives for r-process Nuclei, Nucl. Phys. Rev. **60 34**, 425 (2017). doi: 10.11804/NuclPhysRev.34.03.425

[9] X. P. Zhang, Z. Z. Ren, Q. J. Zhi *et al.*, Systematics of β^--decay half-lives of nuclei far from the β-stable line J. Phys. G: Nucl. Part. Phys. **34**, 2611 (2007). doi: 10.1088/0954-3899/34/12/007

[10] T. Tachibana, M. Yamada, and Y. Yoshida, Improvement of the Gross Theory of β-Decay. II: One-Particle Strength Function, Prog. Theor. Phys. **84**, 641 (1990). doi: 10.1143/PTP.84.641

[11] K. Takahashi, and M. Yamada, Gross Theory of Nuclear β-Decay, Prog. Theor. Phys. **41**, 1470 (1969). doi: 10.1143/PTP.41.1470

[12] H. Nakata, T. Tachibana, and M. Yamada, Gross Theory of Nuclear β-Decay, Nucl. Phys. A **625**, 521 (1997). doi: 10.1016/S0375-9474(97)00413-2

[13] J. Y. Fang, J. Chen, and Z. M. Niu, Gross theory of β decay by considering the spin-orbit splitting from relativistic Hartree-Bogoliubov theory, Phys. Rev. C **106**, 054318 (2022). doi: 10.1103/PhysRevC.106.054318

[14] K. Langanke, and G. Martínez-Pinedo, Nuclear weak-interaction processes in stars, Rev. Mod. Phys. **75**, 819 (2003). doi: 10.1103/RevModPhys.75.819

[15] B. R. Barrett, Microscopic calculations of nuclear structure beyond the 0p-shell, J. Phys.: Conf. Ser. **445**, 012002 (2013). doi: 10.1088/1742-6596/445/1/012002

[16] K. Langanke, E. Kolbe, and D. J. Dean, Unblocking of the Gamow-Teller strength in stellar electron capture on neutron-rich germanium isotopes, Phys. Rev. C **63**, 032801(R) (2001). doi: 10.1103/PhysRevC.63.032801

[17] T. Suzuki, T. Yoshida, T. Kajino *et al.*, β decays of isotones with neutron magic number of N=126 and r-process nucleosynthesis, Phys. Rev. C **85** 015802 (2012). doi: 10.1103/PhysRevC.85.015802

[18] Q. Zhi, E. Caurier, J. J. Cuenca-García *et al.*, Shell-model half-lives including first-forbidden contributions for r-process waiting-point nuclei, Phys. Rev. C **87**, 025803 (2013). doi: 10.1103/PhysRevC.87.025803

[19] Z. M. Niu, Y. F. Niu, H. Z. Liang *et al.*, β-decay half-lives of neutron-rich nuclei and matter flow in the r-process, Phys. Lett. B **723**, 172 (2013). doi: 10.1016/j.physletb.2013.04.048

[20] J. Engel, M. Bender, J. Dobaczewski *et al.*, β decay rates of r-process waiting-point nuclei in a self-consistent approach, Phys. Rev. C **60**, 014302 (1999). doi: 10.1103/PhysRevC.60.014302

[21] D. D. Ni, and Z. Z. Ren, β-decay rates of neutron-rich Zr and Mo isotopes in the deformed quasiparticle random-phase approximation with realistic interactions, Phys. Rev. C **89**, 064320 (2014). doi: 10.1103/PhysRevC.89.064320

[22] P. Sarriguren, β-decay properties of neutron-rich rare-earth isotopes, Phys. Rev. C **95**, 014304 (2017). doi: 10.1103/PhysRevC.95.014304

[23] K. Yoshida, Naturalness, conformal symmetry, and duality, Prog. Theor. Exp. Phys. **11**, 113D02 (2013). doi: 10.1093/ptep/ptt098

[24] F. Minato, and C. L. Bai, Impact of Tensor Force on β Decay of Magic and Semimagic Nuclei, Phys. Rev. Lett. **110**, 122501 (2013). doi: 10.1103/PhysRevLett.110.122501

[25] Z. Y. Wang, Y. F. Niu, Z. M. Niu *et al.*, Nuclear β-decay half-lives in the relativistic point-coupling model, J. Phys. G: Nucl. Part. Phys. **43**, 045108 (2016). doi: 10.1088/0954-3899/43/4/045108

[26] T. Marketin, L. Huther, and G. Martínez-Pinedo, Large-scale evaluation of β-decay rates of r-process nuclei with the inclusion of first-forbidden transitions, Phys. Rev. C **93**, 025805 (2016). doi: 10.1103/PhysRevC.93.025805

[27] Y. F. Niu, Z. M. Niu, G. Colò *et al.*, Interplay of quasiparticle-vibration coupling and pairing correlations on β-decay half-lives, Phys. Lett. B **780**, 325 (2018). doi: https://doi.org/10.1016/j.physletb.2018.02.061

[28] Y. F. Niu, G. Colò, E. Vigezzi *et al.*, Quasiparticle random-phase approximation with quasiparticle-vibration coupling: Application to the Gamow-Teller response of the superfluid nucleus ^{120}Sn., Phys. Rev. C **94**, 064328 (2016). doi: 10.1103/PhysRevC.94.064328

[29] Y. F. Niu, Z. M. Niu, G. Colò *et al.*, Particle-Vibration Coupling Effect on the β Decay of Magic Nuclei, Phys. Rev. Lett. **114**, 142501 (2015). doi: 10.1103/PhysRevLett.114.142501

[30] P. Möller, J.R. Nix, and K.-L. Kratz, Nuclear Properties for Astrophysical and Radioactive Ion-Beam Applications, At. Data Nucl. Data Tables **66**, 131 (1997). doi: 10.1006/adnd.1997.0746

[31] P. Möller, B. Pfeiffer, and K.-L. Kratz, New calculations of gross β-decay properties for astrophysical applications: Speeding-up the classical r process, Phys. Rev. C **67**, 055802 (2003). doi: 10.1103/PhysRevC.67.055802

[32] P. Möller, A. J. Sierk, T. Ichikawa *et al.*, Nuclear ground-state masses and deformations: FRDM(2012), At. Data Nucl. Data Tables **109-110**, 1 (2016). doi: 10.1016/j.adt.2015.10.002

[33] P. Möller, M. R. Mumpower, T. Kawano *et al.*, Nuclear properties for astrophysical and radioactive-ion-beam applications (II), At. Data Nucl. Data Tables **125**, 1 (2019). doi: 10.1016/j.adt.2018.03.003

[34] W. B. He, Q. F. Li, Y. G. Ma *et al.*, Machine learning in nuclear physics at low and intermediate energies, Sci. China Phys. Mech. Astron. **66**, 282001 (2023). doi: 10.1007/s11433-023-2116-0

[35] Z. M. Niu, and H. Z. Liang, Nuclear mass predictions based on Bayesian neural network approach with pairing and shell effects, Phys. Lett. B **778**, 48 (2018). doi: 10.1016/j.physletb.2018.01.002

[36] R. Utama, J. Piekarewicz, and H. B. Prosper, Nuclear mass predictions for the crustal composition of neutron stars: A Bayesian neural network approach, Phys. Rev. C **93**, 014311 (2016). doi: 10.1103/PhysRevC.93.014311

[37] Z. M. Niu, and H. Z. Liang, Nuclear mass predictions with machine learning reaching the accuracy required by r-process studies, Phys. Rev. C **106**, L021303 (2022). doi: 10.1103/PhysRevC.106.L021303

[38] X. H. Wu, L. H. Guo, and P. W. Zhao, Nuclear masses in extended kernel ridge regression with odd-even effects, Phys. Lett. B **819**, 136387 (2021). doi: 10.1016/j.physletb.2021.136387

[39] H. F. Zhang, L. H. Wang, J. P. Yin *et al.*, Performance of the Levenberg–Marquardt neural network approach in nuclear mass prediction, J. Phys. G **44**, 045110 (2017). doi: 10.1088/1361-6471/aa5d78

[40] L. Neufcourt, Y. C. Cao, W. Nazarewicz *et al.*, Neutron Drip Line in the Ca Region from Bayesian Model Averaging, Phys. Rev. Lett. **122**, 062502 (2019). doi: 10.1103/PhysRevLett.122.062502

[41] Z. Y. Yuan, D. Bai, Z. Wang *et al.*, Reliable calculations of nuclear binding energies by the Gaussian process of machine learning, Nucl. Sci. Tech. **35**, 105 (2024). doi: 10.1007/s41365-024-01463-9

[42] R. Utama, W.-C. Chen, and J. Piekarewicz, Nuclear charge radii: density functional theory meets Bayesian neural networks, J. Phys. G: Nucl. Part. Phys. **43**, 114002 (2016). doi: 10.1088/0954-3899/43/11/114002

[43] Y. F. Ma, C. Su, J. Liu *et al.*, Predictions of nuclear charge radii and physical interpretations based on the naive Bayesian probability classifier, Phys. Rev. C **101**, 014304 (2020). doi: 10.1103/PhysRevC.101.014304

[44] D. Wu, C. L. Bai, H. Sagawa *et al.*, Calculation of nuclear charge radii with a trained feed-forward neural network, Phys. Rev. C **102**, 054323 (2020). doi: 10.1103/PhysRevC.102.054323

[45] T. S. Shang, J. Li, and Z. M. Niu, Prediction of nuclear charge density distribution with feedback neural network, Nucl. Sci. Tech. **33**, 153 (2022). doi: 10.1007/s41365-022-01140-9

[46] T. S. Shang, H. H. Xie, J. Li *et al.*, Global prediction of nuclear charge density distributions using a deep neural network, Phys. Rev. C **110**, 014308 (2024). doi: 10.1103/PhysRevC.110.014308

[47] L. Tang, and Z. H. Zhang, Nuclear charge radius predictions by kernel ridge regression with odd–even effects, Nucl. Sci. Tech. **35**, 19 (2024). doi: 10.1007/s41365-024-01379-4

[48] Z. A. Wang, J. C. Pei, Y. Liu *et al.*, Bayesian Evaluation of Incomplete Fission Yields, Phys. Rev. Lett. **123**, 122501 (2019). doi: 10.1103/PhysRevLett.123.122501

[49] C. Y. Qiao, J. C. Pei, Z. A. Wang *et al*., Bayesian evaluation of charge yields of fission fragments of ^{239}U Phys. Rev. C **103**, 034621 (2021). doi: 10.1103/PhysRevC.103.034621

[50] J. H. Bai, Z. M. Niu, B. Y. Sun *et al*., The description of giant dipole resonance key parameters with multitask neural networks, Phys. Lett. B **815**, 136147 (2021). doi: 10.1016/j.physletb.2021.136147

[51] X. H. Wang, L. Zhu, and J. Su, Providing physics guidance in Bayesian neural networks from the input layer: The case of giant dipole resonance predictions, Phys. Rev. C **104**, 034317 (2021). doi: 10.1103/PhysRevC.104.034317

[52] R.-D. Lasseri, D. Regnier, J. P. Ebran *et al*., Taming Nuclear Complexity with a Committee of Multilayer Neural Networks, Phys. Rev. Lett. **124**, 162502 (2020). doi: 10.1103/PhysRevLett.124.162502

[53] Y. F. Wang, X. Y. Zhang, Z. M. Niu *et al*., Study of nuclear low-lying excitation spectra with the Bayesian neural network approach, Phys. Lett. B **830**, 137154 (2022). doi: 10.1016/j.physletb.2022.137154

[54] W. B. He, Y. G. Ma, L. G. Pang *et al*., High-energy nuclear physics meets machine learning, Nucl. Sci. Tech. **34**, 88 (2023). doi: 10.1007/s41365-023-01233-z

[55] B. S. Cai, and C. X. Yuan, Random forest-based prediction of decay modes and half-lives of superheavy nuclei, Nucl. Sci. Tech. **34**, 204 (2023). doi: 10.1007/s41365-023-01354-5

[56] Y. D. Zeng, J. Wang, R. Zhao *et al*., Decomposition of fissile isotope antineutrino spectra using convolutional neural network, Nucl. Sci. Tech. **34**, 79 (2023). doi: 10.1007/s41365-023-01229-9

[57] Y. F. Gao, B. S. Cai, and C. X. Yuan, Investigation of β-decay half-life and delayed neutron emission with uncertainty analysis, Nucl. Sci. Tech. **34**, 9 (2023). doi: 10.1007/s41365-022-01153-4

[58] P. X. Du, T. S. Shang, K. P. Geng *et al*., Inference of parameters for the back-shifted Fermi gas model using a feedforward neural network, Phys. Rev. C **109**, 044325 (2024). doi: 10.1103/PhysRevC.109.044325

[59] Z. P. Gao, and Q. F. Li, Studies on several problems in nuclear physics by using machine learning, Nucl. Tech. **46**, 080009 (2023). doi: 10.11889/j.0253-3219.2023.hjs.46.080009

[60] F. P. Li, L. G. Pang, and X. N. Wang, Application of machine learning to the study of QCD transition in heavy ion collisions, Nucl. Tech. **46**, 040014 (2023). doi: 10.11889/j.0253-3219.2023.hjs.46.040014

[61] J. Zhou, and J. Xu, Bayesian inference of neutron-skin thickness and neutron-star observables based on effective nuclear interactions, Sci. China Phys. Mech. Astron. **67** 282011 (2024). doi: 10.1007/s11433-024-2406-4

[62] R. Wang, Y. G. Ma, R. Wada *et al*., Nuclear liquid-gas phase transition with machine learning, Phys. Rev. Res. **2**, 043202 (2020). doi: 10.1103/PhysRevResearch.2.043202

[63] Y. D. Song, R. Wang, Y. G. Ma *et al*., Determining the temperature in heavy-ion collisions with multiplicity distribution, Phy. Lett. B **814**, 136084 (2021). doi: 10.1016/j.physletb.2021.136084

[64] N. J. Costiris, E. Mavrommatis, K. A. Gernoth *et al*., Decoding β-decay systematics: A global statistical model for β^- half-lives, Phys. Rev. C **80**, 044332 (2009). doi: 10.1103/PhysRevC.80.044332

[65] Z. M. Niu, H. Z. Liang, B. H. Sun *et al*., Predictions of nuclear β-decay half-lives with machine learning and their impact on r-process nucleosynthesis, Phys. Rev. C **99**, 064307 (2019). doi: 10.1103/PhysRevC.99.064307

[66] F. Minato, Z. M. Niu, and H. Z. Liang, Calculation of β-decay half-lives within a Skyrme-Hartree-Fock-Bogoliubov energy density functional with the proton-neutron quasiparticle random-phase approximation and isoscalar pairing strengths optimized by a Bayesian method Phys. Rev. C **106**, 024306 (2022). doi: 10.1103/PhysRevC.106.024306

[67] W. F. Li, X. Y. Zhang, Y. F. Niu *et al*., Comparative study of neural network and model averaging methods in nuclear β-decay half-life predictions, J. Phys. G: Nucl. Part. Phys. **51**, 015103 (2024). doi: 10.1088/1361-6471/ad0314

[68] P. Li, J. H. Bai, Z. M. Niu *et al*., β-decay half-lives studied using neural network method, Sci. China Phys. Mech. Astron. **52**, 252006 (2022). doi: 10.1360/SSPMA-2021-0299

[69] E. M. Ney, J. Engel, T. Li *et al*., Global description of β^- decay with the axially deformed Skyrme finite-amplitude method: Extension to odd-mass and odd-odd nuclei, Phys. Rev. C **102**, 034326 (2020). doi: 10.1103/PhysRevC.102.034326

[70] X. Glorot, and Y. Bengio, Understanding the difficulty of training deep feedforward neural networks, Proc. Mach. Learn **9**, 249 (2010). doi: 10.5555/3157382.3157509

[71] A. E. Hoerl, and R. W. Kennard, Ridge Regression: Applications to Nonorthogonal Problems, Technometrics **12**, 69 (1970). doi: 10.2307/1267352

[72] A. E. Hoerl, and R. W. Kennard, Ridge Regression: Biased Estimation for Nonorthogonal Problems, Technometrics **12**, 55 (1970). doi: 10.1080/00401706.1970.10488699

[73] M. Wang, W. J. Huang, F. G. Kondev *et al*., The AME 2020 atomic mass evaluation (II). Tables, graphs and references, Chin. Phys. C **45**, 030003 (2021). doi: 10.1088/1674-1137/abddaf

[74] J. Liu, Y. F. Niu, and W. H. Long, New magicity N = 32 and 34 due to strong couplings between Dirac inversion partners, Phys. Lett. B **806**, 135524 (2020). doi: 10.1016/j.physletb.2020.135524

[75] G. Lorusso, S. Nishimura, Z. Y. Xu *et al*., β-Decay Half-Lives of 110 Neutron-Rich Nuclei across the N = 82 Shell Gap: Implications for the Mechanism and Universality of the Astrophysical r Process, Phys. Rev. Lett. **114**, 192501 (2015). doi: 10.1103/PhysRevLett.114.192501

[76] N. Wang, M. Liu, X. Z. Wu *et al*., Surface diffuseness correction in global mass formula, Phys. Lett. B **734**, 215 (2014). doi: 10.1016/j.physletb.2014.05.049